Effects of Nonlinear Distortion on CDMA Communication Systems

Seng-Woon Chen, *Senior Member, IEEE,* William Panton, and Robert Gilmore, *Senior Member, IEEE*

***Abstract*—We report a rigorous approach to analyze the effects of nonlinear distortion on code division multiple access (CDMA) wireless communication systems based on time-domain analysis and band-pass nonlinearity theory. Given AM-AM and AM-PM characteristics of a nonlinear device, this technique is capable of predicting adjacent channel power rejection (ACPR), noise power ratio (NPR), two-tone intermodulation products, CDMA waveform quality, and baseband signal vector constellation at the output of the nonlinear device. To demonstrate and verify the capability of this technique, an L-band power amplifier was designed, built, tested with CDMA waveforms, and compared with the simulated results. Excellent agreement between the measured and predicted results has been achieved.**

I. Introduction

IN CELLULAR and personal communication systems (PCS), nonlinear devices, especially the power amplifier (PA), generate co-channel and adjacent channel interference due to intermodulation (IMD) and sideband regrowth. In global satellite communications, stringent regulatory emission requirements in the reverse link have been proposed to prevent interference with existing navigation communication systems. Several different methods have been used to characterize nonlinear distortion of a nonlinear device and to evaluate its effects on RF system performance. Third-order intercept point (IP3) and two-tone IMD products are the most popular specifications. NPR is preferred in transponder design for commercial communication satellites to simulate multi-carrier situation. In cellular and PCS, sideband regrowth or ACPR is favored. In addition, it has been found that output $P_{1\text{dB}}$ of a power amplifier, when measured with band-limited noise like signal, such as CDMA waveform, is usually 1–2 dB below that measured with CW tone. In many cases, the power amplifier must be operated a few dB below $P_{1\text{dB}}$ to be sufficiently linear.

This paper describes a time-domain approach to accurately predict sideband regrowth and power suppression caused by nonlinear devices in CDMA systems based on measurement of AM-AM and AM-PM characteristics and application of band-pass nonlinearity theory and digital signal processing techniques. Since all the calculation is done at baseband, the effect of this distortion to the overall system performance can be analyzed by examining the time-domain envelope waveforms and signal vector constellation. The material presented here will provide insight into the effects of nonlinear distortion to wireless communications and correlation among different nonlinearity specifications.

Manuscript received March 29, 1996.
The authors are with Qualcomm, Inc., San Diego, CA 92121 USA.
Publisher Item Identifier S 0018-9480(96)08576-6.

II. Principles

A. Representation of TIA/EIA/IS-95 CDMA Signals

In cellular, PCS, and mobile satellite communication systems, the bandwidth of each RF channel is much less than the carrier frequency, the RF signal can be represented as

$$\begin{aligned} s(t) &= s_I(t)\cos(\omega_c t) - s_Q(t)\sin(\omega_c t) \\ &= \text{Re}\{[s_I(t) + j s_Q(t)] \cdot e^{j\omega_c t}\} \\ &= \text{Re}[\underline{s}(t) \cdot e^{j\omega_c t}] \end{aligned} \tag{1}$$

where $s_I(t)$ is referred to as the in-phase component of the band-pass signal $s(t)$ and $s_Q(t)$ as the quadrature component of the signal. $\underline{s}(t)$ is the complex envelope of $s(t)$ and is a low-pass baseband signal. Since $\underline{s}(t)$ is complex, its frequency spectrum is not necessarily symmetric. The complex envelope $\underline{s}(t)$ can be expressed in the form

$$\underline{s}(t) = a(t) \cdot e^{j\phi(t)} \tag{2}$$

where $a(t)$ and $\phi(t)$ are both real-valued and low-pass functions.

Let the narrow band band-pass signal $s(t)$ be applied to a linear time-invariant system with impulse response $h(t)$ and transfer function $H(f)$. By analogy to the representation of band-pass signal, we may express $h(t)$ in the form

$$h(t) = \text{Re}[\underline{h}(t) \cdot e^{j\omega_c t}]. \tag{3}$$

It has been shown [1] that the complex envelope $\underline{y}(t)$ of the output signal $y(t)$ is related to the complex envelope $\underline{s}(t)$ of the input signal and the complex impulse response $\underline{h}(t)$ of the band-pass system as follows

$$\underline{y}(t) = \underline{s}(t) \otimes \underline{h}(t) \tag{4}$$

where $\otimes$ is the shorthand notation for convolution. Therefore, the analysis of a band-pass system can be replaced by an equivalent low-pass analysis and retains the essence of the filtering process. By dealing with the baseband signals, application of digital signal processing (DSP) techniques becomes feasible and greatly facilitates the analysis.

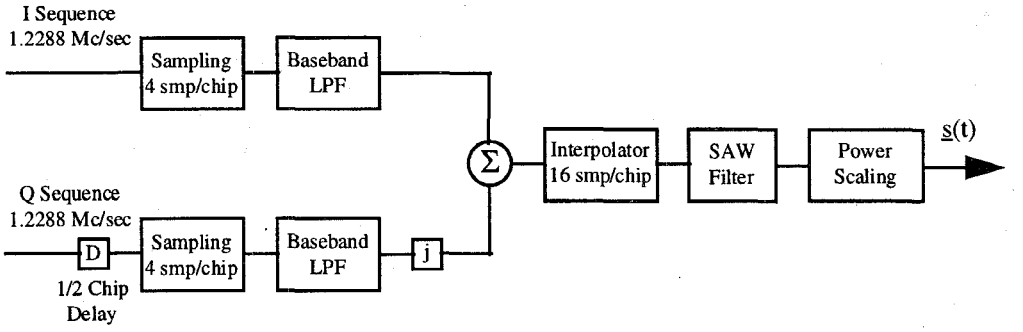

Fig. 1. Simplified model of CDMA reverse traffic channel.

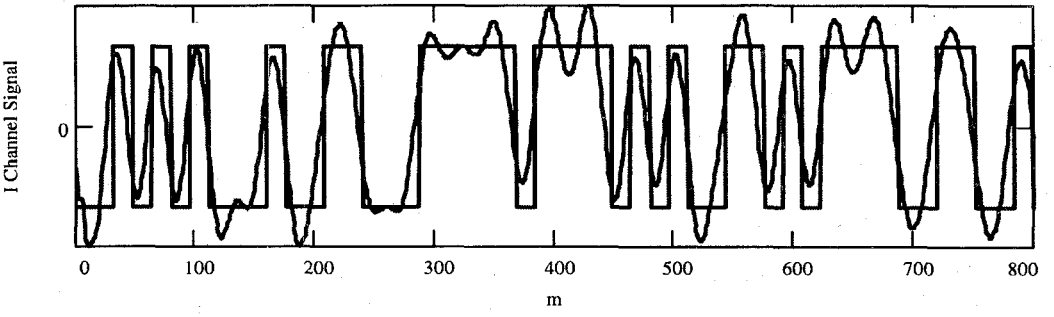

Fig. 2. Simulated I-channel signal for OQPSK modulated CDMA baseband complex envelope.

Fig. 1 shows a simplified block diagram of the CDMA transmitter for the phone to base station link (reverse link). This transmitter is the type specified in TIA/EIA/IS-95 for cellular telephone communication and is used for PCS and global satellite communication systems as well. The digital pseudo-noise (PN) sequences that modulate the I and Q channels are modeled as two independent random number sequences with chip rate 1.2288 Mcps. The impulse response of the FIR baseband filter complies with TIA/EIA/IS-95. Before the data sequences are fed to the digital FIR baseband filters, each sequence is sampled at four times the chip rate as stated in IS-95. In global satellite communications, such as Globalstar, power amplifier sideband regrowth at 5–10 MHz away from the lowest channel carrier frequency has been a major concern to existing navigation systems such as GPS, and GLONASS. Therefore the sequences are up sampled at 16 times the chip rate with interpolation to cover 8 × 1.2288 MHz offset at each side of the carrier frequency according to the Nyquist Theorem. An IF band-pass filter (usually in the form of a SAW filter) follows the OQPSK modulator to reduce the transmit noise floor. Since we are dealing with baseband signals, the IF band-pass filter is frequency-translated to baseband. Because a SAW filter is an FIR filter, it can be simulated digitally. The envelope waveform is scaled to the desired power level prior to being applied to the nonlinear device under analysis. In the generation of the simulated CDMA waveform, the baseband filtering is implemented in the time domain, i.e., convolution of the sampled random sequence with the impulse response of the baseband filter. The baseband filtered sequences are then Fourier transformed using the FFT algorithm and multiplied with the frequency response of the SAW filter. Finally, the CDMA baseband envelope signal is obtained by inverse FFT. Fig. 2 shows a generated OQPSK modulated CDMA baseband envelope waveforms.

B. Band-Pass Nonlinearity

The effect of a memoryless nonlinearity, sandwiched between band-pass filters (BPF) as shown in Fig. 3, on a narrow band waveform was first analyzed by Blackman [2]–[3]. The combined effects of AM-AM, AM-PM conversion, and additive noise in multicarrier TWTA systems were reported by Shimbo [4]. In cellular, PCS and satellite mobile communications, the first band-pass filter may represent the aggregate transfer function of baseband pulse shaping filter and any IF and RF band-pass filters prior to the nonlinear device. The nonlinear distortion generated by an RF high power amplifier is usually of major interest. If a narrow band signal $s(t)$ of (1) is applied to a nonlinear device with nonlinear characteristic function $f(\cdot)$, the nonlinearity will generate intermodulation signals around DC, fc, 2fc, ..., etc. The second BPF selects the signal around fc and rejects the others. Let $y(t)$ be the output of second BPF, then

$$\begin{aligned} y(t) &= \mathrm{Re}[\underline{y}(t) \cdot e^{j\omega_c t}] \\ &= \mathrm{Re}\{[F[a(t)] \cdot e^{j\{\phi(t)+P[a(t)]\}} \cdot e^{j\omega_c t}\} \\ &= \mathrm{Re}\{a(t)G[a(t)] \cdot e^{j\{\phi(t)+P[a(t)]\}} \cdot e^{j\omega_c t}\} \end{aligned} \quad (5)$$

where

$$F(a) = a(t)G[a(t)] = \frac{\pi}{2}\int_0^{\pi} f(a\cos\theta)\cos\theta \, d\theta \quad (6)$$

is the first order Chebyshev transform of the nonlinear characteristic function $f(\cdot)$. From (5), the output complex envelope

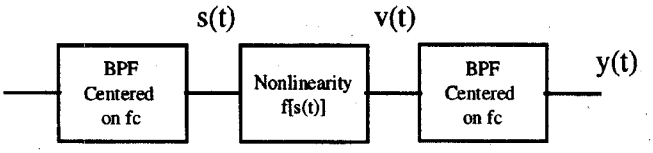

Fig. 3. Bandpass nonlinearity.

$\underline{y}(t)$ is related to the input complex envelope $\underline{s}(t)$ as follows:

$$\begin{aligned}\underline{y}(t) &= F[a(t)] \cdot e^{j\{\phi(t)+P[a(t)]\}} \\ &= a(t)G[a(t)] \cdot e^{j\{\phi(t)+P[a(t)]\}}. \end{aligned} \tag{7}$$

In control theory, $F(a)/a = G(a)$ is called the describing function of the nonlinearity. In RF/Microwave communications, it is known as AM-AM distortion or simply gain versus input power. $P(a)$ is referred to as AM-PM distortion. From (1) and (7), the complex envelope and hence the real-valued signal at a nonlinear device output can be derived from the input waveform and measurement of AM-AM and AM-PM distortion of the nonlinearity. AM-AM and AM-PM of a power amplifier can be measured directly on a network analyzer using a CW power sweep. For narrow band RF communication systems, measurement at a single frequency is usually sufficient.

To predict the effects of nonlinearity on a CDMA system, a baseband complex envelope for the CDMA signal is first generated and scaled. In generation of $\underline{s}(t)$, 256 bits of digital data are generated for each I and Q channel independently using two random number generators. Each bit of 0 is represented by -1 V, and 1 is represented by 1 V. Since 256 chips are generated for each channel, the complex envelope $\underline{s}(t)$ is represented by a discrete complex sequence $\underline{s}[n]$ of $N = 16 \times 256 = 4096$ samples. Using the measured AM-AM and AM-PM distortion and generated complex envelope samples $\underline{s}[n]$, the output complex envelope sequence $\underline{y}[n]$ of the PA can be derived from (7). Adjacent channel power rejection (ACPR) or sideband regrowth of the power amplifier output can be obtained with power spectrum analysis [5]

$$S_{\underline{y}}[k] = \frac{|\underline{Y}[k]|^2}{N^2} \qquad k = 0, 1, \cdots N-1 \tag{8}$$

where $S_y[k]$ is the power spectral density (PSD) of $\underline{y}[n]$ over the resolution bandwidth $Rb = 16 \times 1.2288/4096 = 4.8$ kHz, and $\underline{Y}[k]$ is the FFT of $\underline{y}[n]$, i.e.

$$\begin{aligned}\underline{Y}[k] &= \mathrm{FFT}(\underline{y}[n]) = \sum_{n=0}^{N-1} \underline{y}[n] \cdot e^{j2\pi k(n/T)} \\ & k = 0, 1, \cdots N-1. \end{aligned} \tag{9}$$

The output power P_{out} of power amplifier can be calculated as follows

$$P_{\text{out}} = 10 \log \left[\frac{1}{N} \sum_{n=0}^{N-1} |\underline{y}[n]|^2 \right] = 10 \log \left[\frac{1}{N} \sum_{k=0}^{N-1} |\underline{Y}[k]|^2 \right]. \tag{10}$$

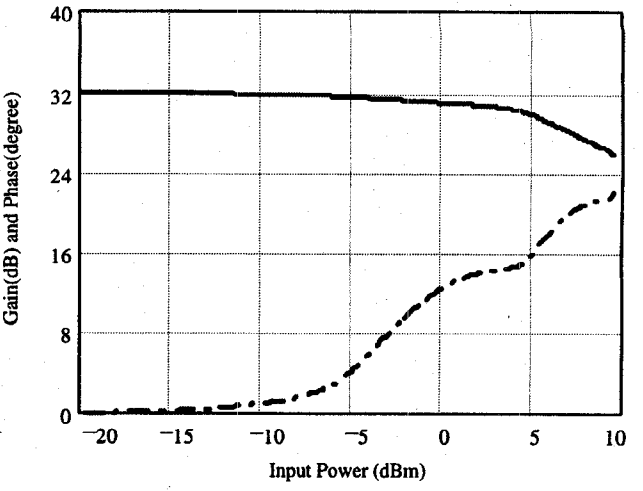

Fig. 4. Measured AM-AM (solid line) and AM-PM (dash-dot line) of an L-band power amplifier.

III. Simulation and Measurement Results

A. ACPR and Power Suppression of CDMA Modulation

To demonstrate the capability of the IMD simulation technique, we designed, built, and tested an L-band two-stage hybrid power amplifier using Fujitsu's FLL011ME as the first stage device and FLL351ME for the second stage. Fig. 4 shows the AM-AM and AM-PM of the PA measured with the built-in CW power sweep function of the HP8753D network analyzer. For accurate simulation on the compressed region, the CW power sweep has to extend to at least 5 dB beyond $P_{1\text{dB}}$ to account for the peaks in the baseband envelope signal due to baseband pulse-shaping filtering. Fig. 5 shows the predicted and measured output power spectrum density over 16 MHz bandwidth at input powers of 1 and 5 dBm. The measurement is made using the HP8920A RF Communications Test Set with the HP83203A CDMA Cellular Adapter to generate the reverse link CDMA waveform. Adjacent channel power rejection and RF emission at any frequency offset within the simulation bandwidth can be easily seen from the PSD plots. Fig. 6(a) and (b) presents the PSD at 2 and 5 MHz offset from the carrier frequency, respectively. Excellent agreement between the predicted and measured results has been achieved as show in the figures. Fig. 7 shows comparison of simulated with measured P_{out}-P_{in} transfer curves with CW carrier and CDMA signal. At low input power drive, the PA is operating on the linear region so the gain is amplitude-invariant and the CDMA output power is the same as measured from CW carrier. At higher power drive, the gain is more compressed at the time instant when the envelope waveform exhibits peaks due to baseband filtering. From (7), it is apparent that power suppression of the CDMA waveform depends on AM-AM distortion and peak-to-average ratio of the envelope signal.

B. CDMA Signal Constellation and Distortion in Time-Domain

The effects of nonlinear distortion generated by a power amplifier can be visualized with the time-domain waveforms.

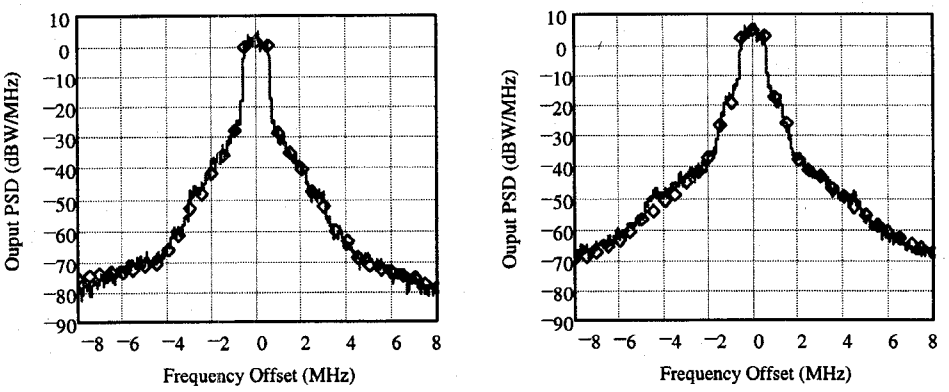

Fig. 5. Power spectrum density curves at output of the PA (a) $P_{\text{in}} = 1$ dBm, $P_{\text{out}} = 31.9$ dBm. (b) $P_{\text{in}} = 5$ dBm, $P_{\text{out}} = 34.3$ dBm; carrier frequency = 1610.875 MHz. (Solid lines: simulation, diamonds: measurement.)

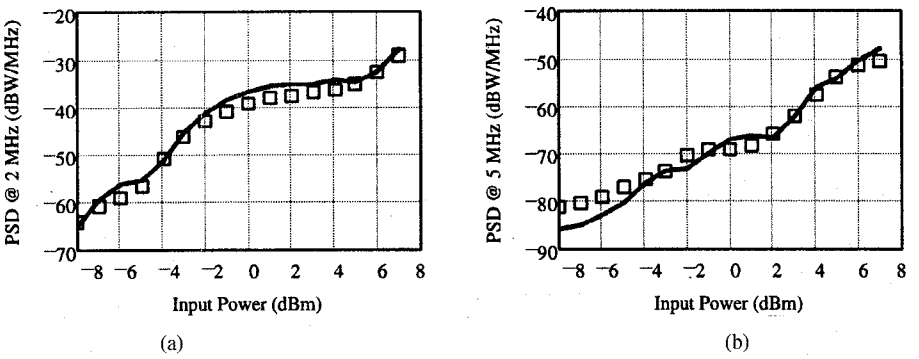

Fig. 6. Power spectrum density at (a) 2 MHz offset and (b) 5 MHz offset as a function of input power. Carrier frequency = 1610.875 MHz. (Solid lines: simulation, squares or boxes: measurement.)

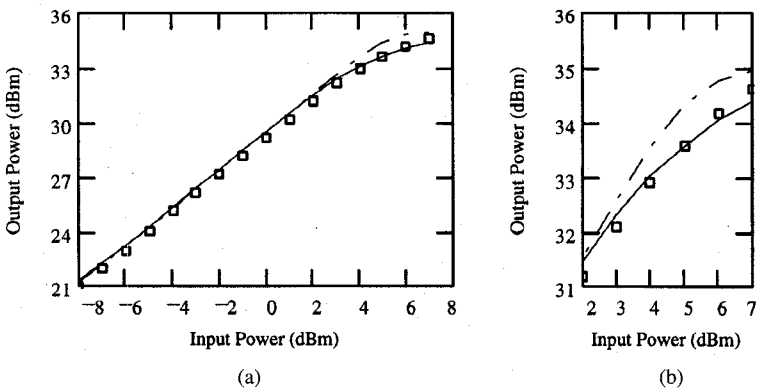

Fig. 7. (a) Pout vs. Pin transfer function. (b) Zoom-in of (a) near compression. (Solid line: CDMA predicted, boxes: CDMA measured, dash-dot: CW)

Fig. 8(a) and (b) shows the input and output time-domain I-channel waveforms for the power amplifier at input drive of 1 dBm and 7 dBm, respectively. Distortion of the baseband signals in the form of amplitude clipping and intersymbol interference can be easily seen from the figures. Distortion of the signal can also be presented in a signal constellation diagram. Fig. 9 shows the QPSK signal constellation at the input and output of the PA when the input drive is equal to 7 dBm. No timing error is assumed in this simulation. In Fig. 9(b), the signal is compressed inwards due to amplitude distortion and rotated and spread due to phase distortion. If large number of chips is simulated, at some time instants, the signal points may move from one quadrant to another and cause bit errors.

In CDMA wireless communication systems, an important measure of the transmitted signal is called CDMA waveform quality ρ which is defined as

$$\rho = \frac{\left|\sum_k \underline{r}[k]\underline{y}[k]^*\right|^2}{\sum_k |\underline{r}[k]|^2 \sum_k |\underline{y}[k]|^2} \tag{11}$$

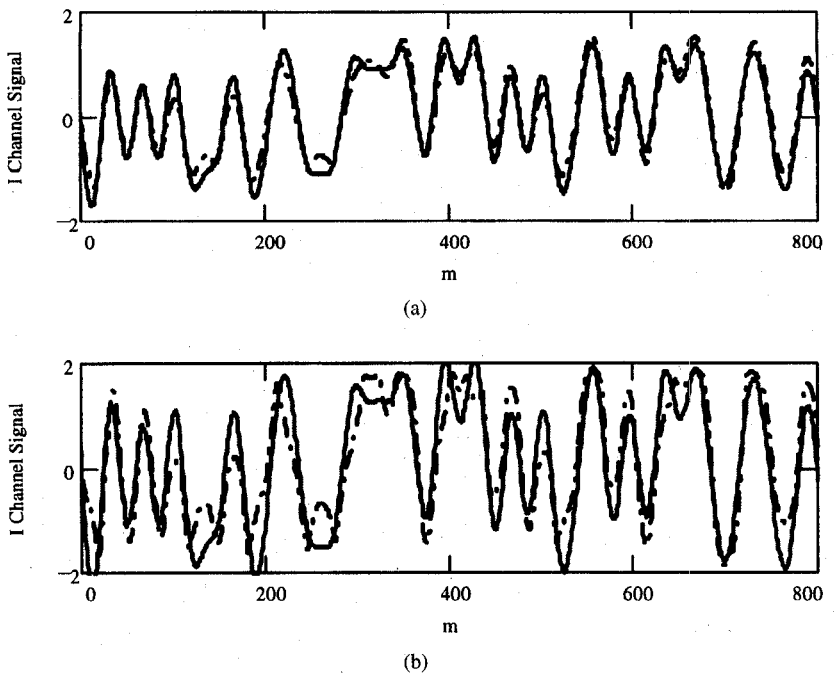

Fig. 8. Input and output CDMA I-channel signals. (a) Input power = 1 dBm. (b) Input power = 7 dBm. (Solid-line: input, dash-dot: output)

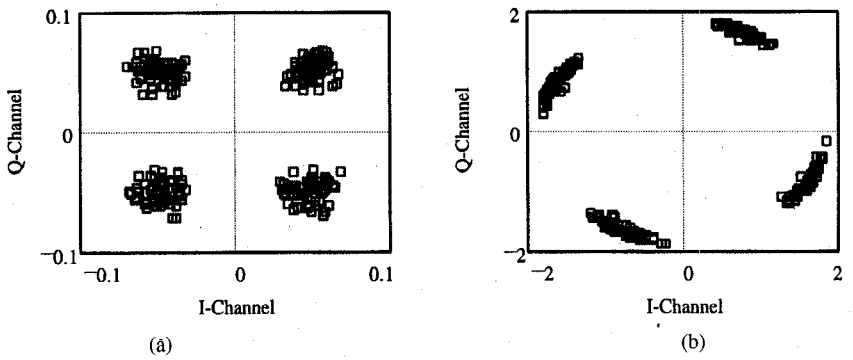

Fig. 9. (a) Input and (b) output signal vector constellation, PA input power = 7 dBm.

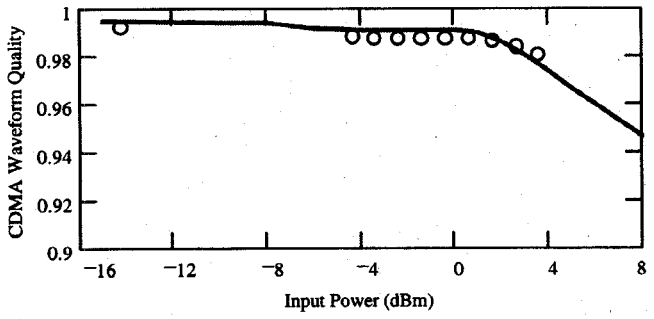

Fig. 10. CDMA waveform quality (ρ) as a function of input power. (Solid-line: simulation, circles: measured)

and is the correlation coefficient between the sampled waveforms $\underline{r}[k]$ and $\underline{y}[k]$. $\underline{y}[k]$ is the complex envelope waveform of the transmitter signal and $\underline{r}[k]$ is that of the ideal waveform at the output of baseband filter as shown in Fig. 1 and serves as the reference waveform. According to TIA/EIA/IS-95 standard, the minimum required ρ is equal to 0.944. Fig. 10

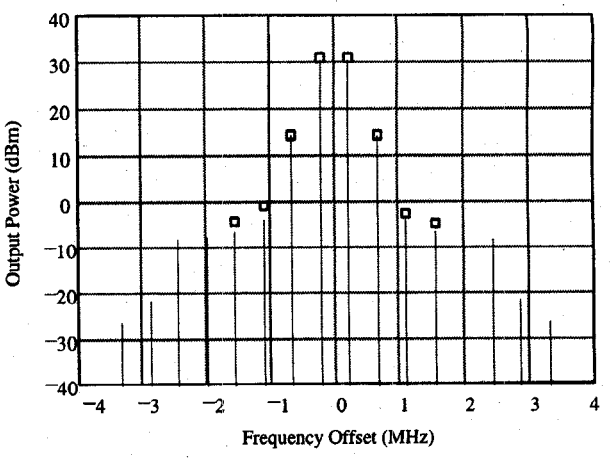

Fig. 11. Measured and predicted two-tone intermodulation products; center frequency = 1618.25 MHz, frequency spacing = 442.5 kHz, total P_{in} = 4.91 dBm, PA nonlinear distortion as shown in Fig. 4. (Solid-line: simulation, box: measured)

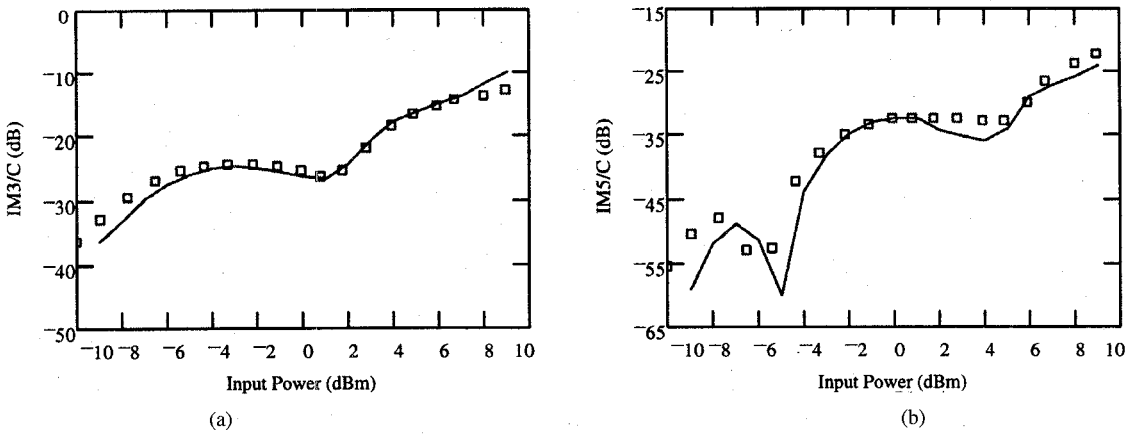

Fig. 12. (a) Carrier to third-order IMD ratio. (b) Carrier to fifth-order IMD ratio. (Solid-lines: simulation, boxes: measurement)

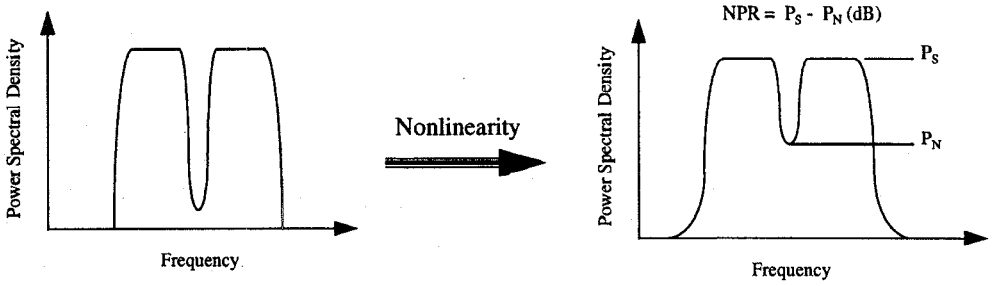

Fig. 13. Noise power ratio (NPR) measurement.

shows the effect of PA's nonlinearity on CDMA waveform quality.

C. Two-Tone Intermodulation

In analogy to band-pass representation for CDMA waveform, two CW carriers, at frequencies ω_1, and ω_2, can be expressed as

$$\begin{aligned} s(t) &= \mathrm{Re}[A(e^{j\omega_1 t} + e^{j\omega_2 t})] \\ &= \mathrm{Re}[2A\cos(\Delta\omega t)\cdot e^{j\omega_c t}] \\ &= \mathrm{Re}[\underline{s}(t)\cdot e^{j\omega_c t}] \end{aligned} \tag{12}$$

where $\Delta\omega = (\omega 2 - \omega 1)/2$ and $\omega c = (\omega 2 + \omega 1)/2$. It is assumed (but not necessary) that the two CW tones have identical power of $A^2/2$. From (12), the complex envelope of two tones is a real-valued cosine signal of frequency $(\omega 2 - \omega 1)/2$. Generation of the real-valued cosine signal is straightforward. According to Nyquist Theorem, the sampling rate for the cosine envelope has to be greater than $(\omega 2 - \omega 1)/2\pi$. However, higher sampling rate is required to be able to see higher-order intermodulation products. Using (7), a complex envelope $\underline{y}(t)$ can be obtained from the measured amplitude and phase distortion. The discrete power spectra is then calculated using the FFT algorithm. Fig. 11 shows simulated and measured two-tone intermodulation products for the PA with nonlinear distortion of Fig. 4. Frequency spacing between the carriers is 442.5 kHz, center frequency is 1618.25 MHz, and the total input power is 4.91 dBm. Variations of carrier to third and fifth order intermodulation ratios with input power are simulated, and compared with the measurement and shown in Fig. 12 for the PA nonlinear distortion shown in Fig. 4.

D. Noise Power Ratio (NPR)

NPR measurement has been widely used in satellite communications to evaluate the power amplifier's maximum spurious free dynamic range when the transmission signal includes multiple carriers. NPR measurement requires a complex test setup and test procedures. In the classical approach, a broadband noise source is generated and a high-Q band-stop filter is used to eliminate a portion of the power spectrum at the frequency of interest. NPR is the difference between power levels at the notch frequency with and without the notch filter as shown in Fig. 13. The NPR measurement usually depends on the noise source bandwidth and the notch filter need to be high-Q and narrow band to minimize perturbation to the original broadband noise.

By means of the concept of equivalent gain [6], the output envelope waveform $\underline{y}(t)$ can be represented as

$$\underline{y}(t) = \alpha \underline{s}(t) + \underline{\eta}(t). \tag{13}$$

The essence of equivalent gain is that the nonlinearity output $\underline{y}(t)$ can be represented as summation of undistorted components plus a residual function $\underline{\eta}(t)$. In other words, the input signal $\underline{s}(t)$ passes through the nonlinear device with a fixed gain and phase shift called equivalent gain α and $\underline{\eta}(t)$ can be thought as the intermodulation noise process generated by the nonlinearity. The equivalent gain depends on the baseband envelope waveform and the power amplifier nonlinear characteristics, i.e., AM-AM and AM-PM distortion. By applying the orthogonality constraint, i.e., cross correlation of $\underline{\eta}(t)$ and $\underline{s}(t)$ is equal to zero

$$E[\underline{\eta}(t)\cdot \underline{s}^*(t)] = 0. \tag{14}$$

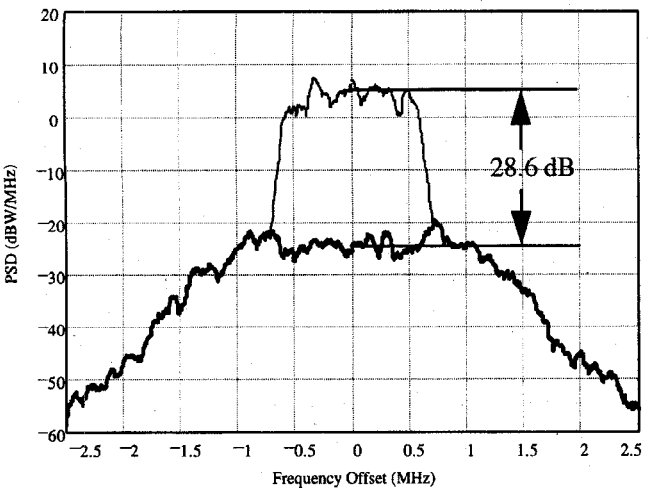

Fig. 14. Predicted noise power ratio for a 1.23 MHz noise loaded waveform. (NPR = 28.6 dB, center frequency = 1618.25 MHz, $P_{\text{in}} = 3.0$ dBm)

The equivalent gain α can be expressed as follows:

$$\alpha = \frac{E[\underline{y}(t) \cdot \underline{s}^*(t)]}{E[\underline{s}(t) \cdot \underline{s}^*(t)]}. \tag{15}$$

Substitute (15) into (13), the intermodulation process $\underline{\eta}(t)$ can be extracted by subtracting $\underline{y}(t)$ from $\alpha \cdot \underline{s}(t)$. By using the DSP techniques described in (8)–(10), the power spectral density for the intermodulation-only process ((t) can be easily derived and the NPR can be obtained by simply comparing the PSD of $\underline{y}(t)$ and $\underline{\eta}(t)$, respectively, as shown in Fig. 14. Since the CDMA signal is a broadband (1.23 MHz) noise-like waveform, it is used to simulate the broadband noise source in NPR simulation. In essence, with AM-AM and AM-PM characteristics, the complicated NPR measurement can be predicted with band-pass nonlinearity theory by introducing the equivalent gain concept without using any band reject filter.

IV. Conclusion

We have demonstrated a time domain approach to analyze nonlinear distortion based on band-pass nonlinearity theory and digital signal processing techniques. The analysis technique has been implemented with Math Soft's Mathcad. To demonstrate the capability of the IMD simulation technique, we designed and built an L-band two-stage hybrid power amplifier. Measurement on power spectrum density and power suppression has been performed with CDMA waveforms to verify the analysis and shows excellent agreement. The effects of PA's nonlinearity on the overall RF communication system performance were visualized by examining the distorted time-domain waveforms and signal vector constellation, and CDMA waveform quality.

The analysis technique described here applies not only to power amplifiers but also to any other nonlinear components such as mixers and switches. This approach can also be used to predict IMD products and NPR. The approach is also well suited to analyze nonlinear distortion in base station and satellite transponder power amplifiers, where the input signals are usually multiple-channels with a different power level for each channel.

References

[1] S. Haykin, *Communication Systems*. New York: Wiley, 1983, 2nd ed.
[2] N. M. Blackman, "Band-pass nonlinearities," *IEEE Trans. Inform. Theory*, vol. IT-10, pp. 162–164, Apr. 1964.
[3] ——, "Detectors, bandpass nonlinearities, and their optimization: Inversion of the chebyshev transform," *IEEE Trans. Inform. Theory*, vol. IT-17, pp. 398–404, July 1971.
[4] O. Shimbo, "Effects of intermodulation, AM-PM conversion, and additive noise in multicarrier TWT systems," *Proc. IEEE*, vol. 59, pp. 230–238, Feb. 1971.
[5] A. V. Oppenheim and R. W. Shafer, *Discrete-Time Signal Processing*. Englewood Cliffs, NJ: Prentice Hall, 1989.
[6] D. S. Arnstein, "Power division in spread spectrum systems with limiting," *IEEE Trans. Commun.*, vol. COM-27, pp. 574–582, Mar. 1979.

Seng-Woon Chen (S'87–M'90–SM'95) received the B.S. degree from National Taiwan University, Taipei, Taiwan, in 1982 and the M.S. and Ph.D. degrees from the University of Maryland, College Park, in 1988 and 1990, respectively, all in electrical engineering.

From 1982 to 1984, he served in the Army Military Police Headquarters, Taipei, Taiwan, as a Second Lieutenant Technical Officer. In 1984, he spent two years as a member of technical staff at Microelectronics Technology Inc., Hsin-Chu, Taiwan, where he was engaged in the development of 18 and 23 GHz microwave digital radios for short-haul relays. From 1986 to 1990, he held a Graduate Research Assistantship with the Microwaves Laboratory, University of Maryland, where he performed research on analysis and modeling of dielectric loaded waveguides, resonators, filters, and periodic structures. From 1990 to 1993, he was a senior system engineer at COMSAT Systems Division where he was involved in the analysis and development of INTELSAT earth stations and INMARSAT mobile terminals, and a senior member of technical staff at COMSAT Laboratories, where his research mainly dealt with microwave and millimeter-wave integrated circuits design and modeling. He spent one year as a senior MMIC development engineer at Martin Marietta Laboratories, Syracuse, NY. Since 1994, he has been with Qualcomm Inc., San Diego, CA, where he is a staff engineer and is responsible for RF systems analysis and components design for various CDMA wireless communication systems. He is currently engaged in the development of user terminals for Globalstar LEO satellite communications. He has authored or coauthored more than 40 technical publications and holds one patent in the areas of electromagnetics, microwave and millimeter-wave devices modeling, MIC/MMIC, filters, and communication systems.

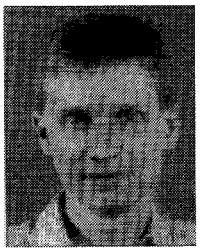

William Panton received the B.S. degree in electrical engineering from the University of Texas, Austin, in 1984. He received the M.S. and Ph.D degrees in electrical engineering from the University of Wisconsin, Madison, in 1991 and 1993, respectively.

Following the B.S. degree through 1987, he held the position of Engineer at Texas Instruments, Dallas. During that time he worked in production support and development of various hybrid technology based mixer and oscillator assemblies operating from X band through Ku band. He began graduate research in the area of Applied Physics and Electromagnetic Theory at the University of Wisconsin in 1987. His Masters' research concerned the analysis of the noise behavior of GaAs FET distributed amplifiers. This theme continued through his Ph.D. research regarding the noise performance of active receiving antenna arrays using distributed amplifier style feed networks. The research included antenna and active feed analysis, noise analysis, fabrication, and testing of various receiving antenna arrays. He joined Qualcomm Inc., San Diego, CA, in 1993. He is currently a Staff Engineer/Manager responsible for the specification, development, and design of the RF aspects of hand held, mobile, and fixed position user terminals for the Globalstar satellite communications system.

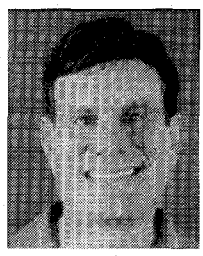

Robert Gilmore (SM'91) received the B.S. and M.S. degrees from the Massachusetts Institute of Technology, Cambridge, in 1976 and 1977, respectively.

He joined Qualcomm, Inc., San Diego, CA, in October 1985. At Qualcomm, he has been involved in the design and technical management of microwave communications terminals, cellular infrastructure equipment, and subscriber products. Most recently, he has been co-Project Engineer for the Ground Segment of the Globalstar LEO Satellite System, as well as Sr. Vice President, Engineering. From 1984 to 1985, was the Director of Engineering at ComStream Corp., San Diego, CA, where his responsibilities included project management and circuit design. He was with M/A-COM LINKABIT Corporation, San Diego, from 1978 to 1984, during which time he rose to the position of Staff Engineer/Manager. His responsibilities included project management and design for military communications systems. From 1974 to 1977, he was involved in the Electrical Engineering cooperative program between the Massachusetts Institute of Technology and Bell Laboratories. He holds three patents in the area of frequency synthesizer design, and is the author of numerous technical publications.

Mr. Gilmore is a member the Tau Beta Pi, Sigma Xi, and Eta Kappa Nu honorary societies.